

Tension and shear block failure of bolted gusset plates¹

Bino B.S. Huns, Gilbert Y. Grondin, and Robert G. Driver

Abstract: Despite the large database of test results for tension and shear block failure in gusset plates, the exact progression of the failure mechanism is not clear. Although current design equations predict the capacity of gusset plates fairly well, it is important for a design equation to not only predict the capacity reliably but also reflect the failure mode accurately. Recent experimental and numerical research has indicated that current design equations do not always predict the failure behaviour accurately. A finite element model was therefore developed to predict the sequence of events that leads to the tear-out of a block of material from a bolted gusset plate in tension. The model was developed to provide a useful tool for studying tension and shear block failure in gusset plates and other structural elements. This paper presents the development of the finite element model and procedure for prediction of tension and shear block failure in gusset plates. Making use of the finite element model, the database of test results is also expanded to include gusset plates with a larger number of transverse lines of bolts than what has been obtained experimentally. A reliability analysis is used to assess several design equations, including the equation adopted in CAN/CSA-S16-01 and a unified equation proposed recently for several types of bolted connections. From this work, a limit states design equation is proposed for gusset plates.

Key words: gusset plate, limit states design, reliability, shear rupture, tension rupture, finite element analysis, failure criterion.

Résumé : Malgré la grande base de données de résultats d'essais sur la défaillance en tension et en cisaillement du bloc des plaques goussets, la progression exacte du mécanisme de rupture n'est pas claire. Bien que les équations de calculs actuelles prédisent la capacité des plaques goussets relativement bien, il est important qu'une équation de calcul non seulement prédisent la fiabilité de la capacité, mais reflète précisément le mode de défaillance. La recherche récente, expérimentale et numérique, indique que les équations de calcul actuelles ne prédisent pas toujours précisément le comportement de rupture. Un modèle d'éléments finis a donc été développé pour prédire la séquence d'événements qui mène à l'arrachement d'un bloc de matériel d'une plaque gusset boulonnée en tension. Le modèle a été développé pour fournir un outil utile pour étudier la défaillance du bloc en cisaillement et en tension dans la plaque gusset et d'autres membres structuraux. Cet article présente le développement d'un modèle d'éléments finis et la procédure pour prédire la défaillance du bloc en tension et en cisaillement des plaques goussets. En se servant du modèle d'éléments finis, la base de données des résultats d'essais est aussi étendue pour inclure les plaques goussets ayant un plus grand nombre de lignes transversales de boulons que ce qui a été obtenu expérimentalement. Une analyse de fiabilité évalue plusieurs équations de calcul, y compris l'équation adoptée dans la norme CSA-S16-01 et une équation unifiée proposée récemment pour plusieurs types de raccords boulonnés. Ce travail a servi de base pour proposer une équation de calcul aux états limites pour les plaques goussets.

Mots clés : plaque gusset, calcul aux états limites, fiabilité, rupture en cisaillement, rupture en tension, analyse par éléments finis, critère de rupture.

[Traduit par la Rédaction]

Introduction

Gusset plates are widely used in steel structures, such as trusses and braced frames in buildings, to transfer forces be-

tween axially loaded members. The design of gusset plates is well established for the transfer of both tension and compression forces (Kulak et al. 1987). One of the failure modes observed in gusset plates loaded in tension consists of tear-

Received 1 December 2004. Revision accepted 3 November 2005. Published on the NRC Research Press Web site at <http://cjce.nrc.ca> on 19 May 2006.

B.B.S. Huns. UMA Engineering Ltd., 17007-107 Avenue, Edmonton, AB T5S 1G3, Canada.

G.Y. Grondin² and R.G. Driver. Department of Civil and Environmental Engineering, University of Alberta, Edmonton, AB T6G 2G7, Canada.

Written discussion of this article is welcomed and will be received by the Editor until 31 August 2006.

¹This article is one of a selection of papers published in this Special Issue on Steel Research.

²Corresponding author (e-mail: ggrondin@ualberta.ca).

ing of a block of material in a combination of tension rupture plus shear yield or rupture, hence the designation tension and shear block failure. Although somewhat misleading from a phenomenological point of view, this failure mode is commonly referred to in the literature as block shear. Although this mode of failure could occur in welded or in bolted connections, it is more common in the latter because of the reduced area that results from the presence of the bolt holes.

Many researchers have used full-scale testing to investigate tension and shear block failure of gusset plate. Chakrabarti and Bjorhovde (1983) and Hardash and Bjorhovde (1984) looked at the inelastic behaviour of gusset plate connections in tension. From their tests and those of other investigators, a model was proposed for predicting the ultimate capacity of gusset plate connections in tension. Their work supported a model in which the ultimate strength of the gusset plate is the sum of the tensile strength of the net area between the bolts in the last row and the shear strength along the connection length. The proposed effective shear stress along the connection length at the ultimate capacity of the connection lies between the shear yield and ultimate strengths and is an inverse function of the length of the connection.

Gusset plate research at the University of Alberta includes investigations of gusset plates in compression by Hu and Cheng (1987) and Yam and Cheng (1993) and of gusset plates under cyclic loading by Rabinovitch and Cheng (1993), Walbridge et al. (1998), and Nast et al. (1999). The experimental work by Rabinovitch and Cheng and by Nast et al. showed tensile failures in the form of tension fracture of the plate material between the holes at the last row of bolts. The connections were not loaded to fracture on the shear planes.

An extensive test program on splice plates in tension was conducted by Udagawa and Yamada (1998). The parameters investigated were the gauge length, end distance, number of lines and rows of bolts, and steel grade. The test specimens were loaded in tension only, and as a result, several specimens failed by tension and shear block. As in earlier test programs, the load sharing between the shear and tension planes and the exact sequence of the failure process were not closely examined.

A review of North American, European, and Japanese practice for tension and shear block design (Kulak and Grondin 2000, 2001) indicated that although the equations in design standards generally give a good prediction of the capacity of gusset plate connections, the models do not predict the failure mode reliably. The Japanese design standard that was the object of the review was found to provide a very conservative estimate of the capacity. A model consisting of rupture on the net tension area and yielding on the gross shear area of the block of material tearing out was proposed by Kulak and Grondin (2001). CAN/CSA-S16-01 (CSA 2001) adopted this model but with a modification that limited the capacity in shear to the rupture capacity on the net shear area. Such an approach, borrowed from the procedure for design of tension members, may not fully describe the true behaviour of gusset plates.

The main objective of the research presented in this paper was to develop a finite element procedure to predict the be-

haviour of tension and shear block failure from initial yielding of the gusset plate to rupture along the tension face and subsequent rupture along the shear faces. Such a model is valuable for the investigation of tension and shear block failure in other members, such as angles, tees, and coped beams. A second objective was to conduct a reliability analysis of the extensive database of test results on gusset plate connections to assess current design equations in a limit states design context and propose a suitable design equation that is consistent with the actual failure mode.

Experimental program

Test specimens

Many laboratory experiments have been conducted to study tension and shear block failure of gusset plates. These experiments were not designed to directly observe the mechanisms leading to failure. A limited experimental program was therefore conducted (Huns et al. 2002) to observe the failure progression in order to add to our understanding of this failure mode and to validate the finite element model.

Two connection configurations were investigated, namely, a long and narrow connection and a short and wide connection. All specimens were fabricated from a grade G40.21-300W steel plate of 6.4 mm (1/4 in.) nominal thickness. The long and narrow connection, illustrated in Fig. 1a, consists of six 19 mm (3/4 in.) A325 bolts and uses the minimum gauge distance allowed in CAN/CSA-S16-01 (CSA 2001), namely, 2.7 times the bolt diameter (51 mm). The bolt holes in the test region were drilled to 20.6 mm, and all the bolts were installed in the snug-tight condition. The bolt pitch was 76 mm. The net tension to shear area ratio for this series of tests was 0.11. The test specimens from this series were designated T1A, T1B, and T1C. One configuration of the short and wide connection, shown in Fig. 1b, consisted of four bolts and used a gauge distance equal to 8.0 times the bolt diameter (152 mm). The test plate had a thickness of 6.5 mm and the bolt pitch was 51 mm, making the net tension to shear area ratio 1.4. This test specimen, designated T2A, failed by shear failure (bolt tear-out) of the plate, with no sign of yielding on the tension face, rather than by tension and shear block failure (Fig. 2). The connection was therefore modified by the addition of a row of four bolts, as shown in Fig. 1c. The modified connection had eight bolts with gauge and pitch dimensions of 51 mm, thus making the net tension to shear area ratio 0.60. The average measured plate thickness for the two specimens of this connection configuration, designated T2B and T2C, was 6.6 mm. All gusset specimens were cut from the same plate.

Test procedure

The intent of the test was to closely examine the process of tension and shear block failure from the yielding stage to fracture along the tension and shear faces of the block. This required the removal of the splice plates at regular intervals during testing to observe the progression of failure. Tests T1A, T1C, T2A, and T2B were conducted this way. To assess the effect of periodic unloading and removal of the splice plates on the behaviour of the test specimens, control tests T1B and T2C were conducted continuously without removal of the splice plates. It was found that periodic re-

Fig. 1. Configuration of test specimens (a) T1A, T1B, T1C, (b) T2A, and (c) T2B and T2C. Dimensions in millimetres.

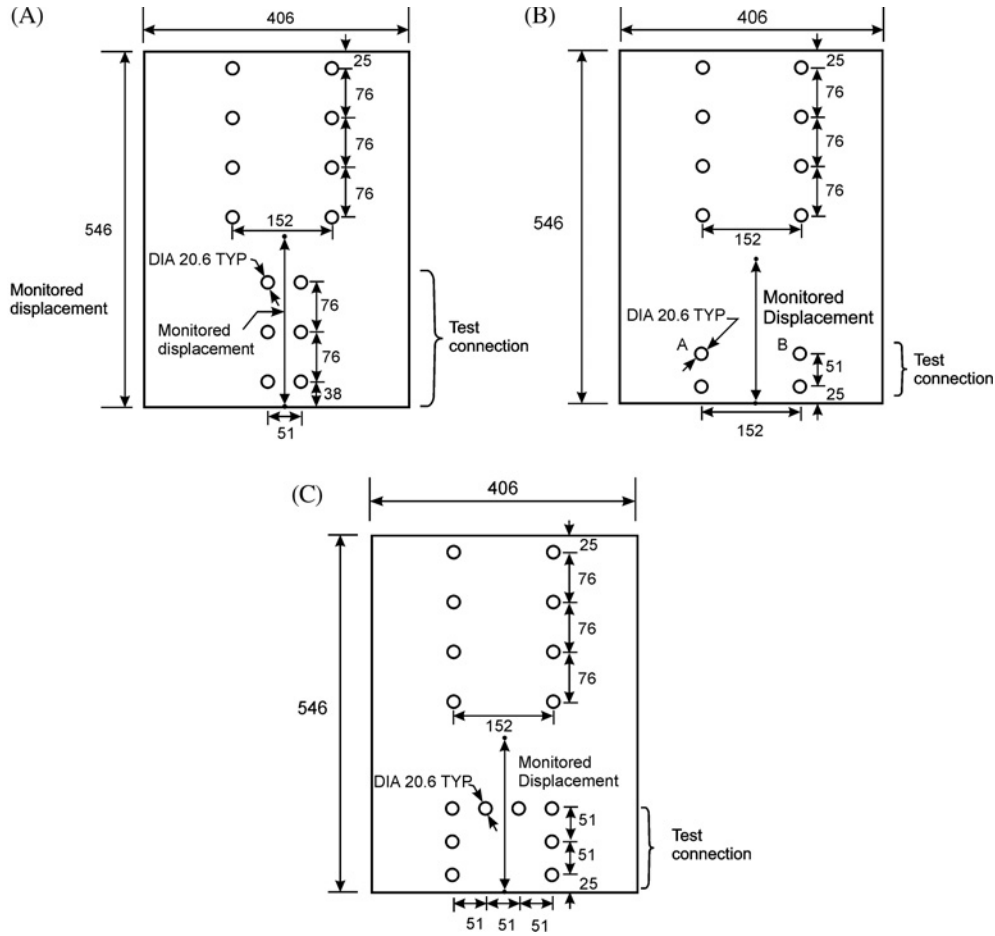
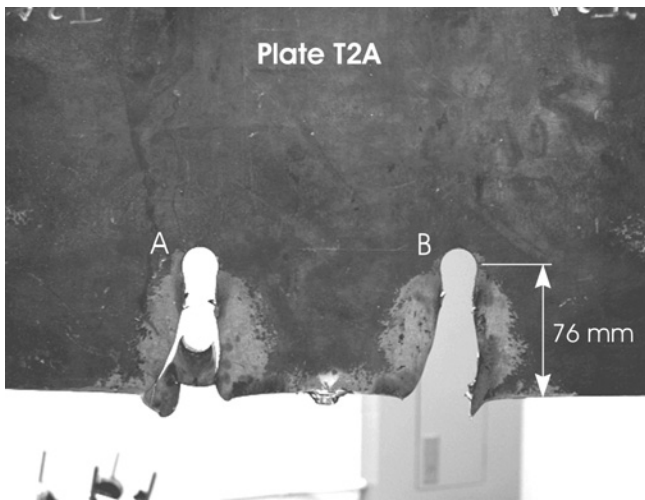


Fig. 2. Shear failure of specimen T2A.



removal of the splice plates during testing did not have a significant impact on the behaviour.

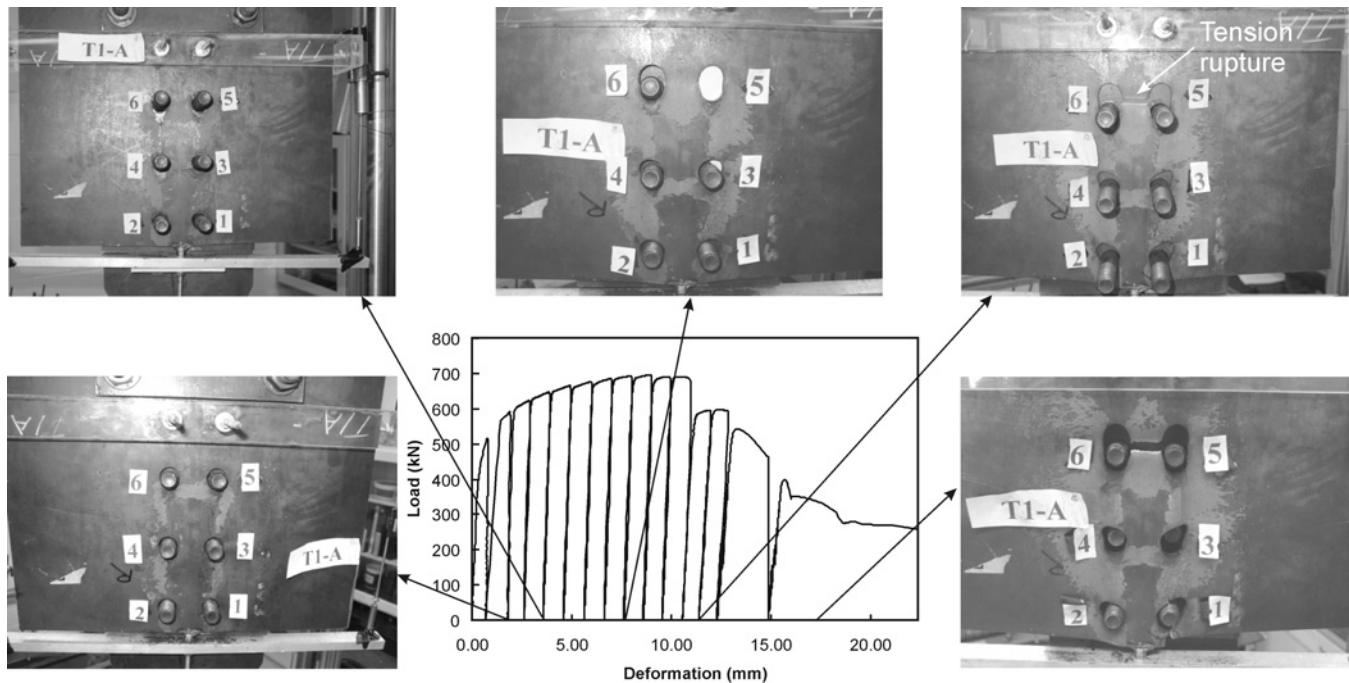
During testing, the deformation of each test specimen was measured over a 250 mm gauge length, the extent of which is indicated in Fig. 1. Finite element analyses of the test specimens prior to testing (Huns et al. 2002) indicated that the displacement at which fracture would initiate was about

2 mm for the specimens of the T1 series and 0.35 mm for specimen T2A. This information was used to establish the magnitude of the unloading intervals so that the fracture process could be observed in detail. A visual inspection of the tension and shear faces in the expected failure zone was conducted at every unloading cycle.

Test results

The test results were obtained in the form of load versus deformation curves for each test specimen. Furthermore, a detailed photographic record of the failure process was collected for each of the four tests that were unloaded periodically. This information has been presented in detail elsewhere (Huns et al. 2002). Figure 3 shows a typical load versus deformation curve for one of the test specimens (T1A) that was loaded cyclically to observe the tension and shear block failure progression. All the test specimens that failed by tension and shear block failure failed by tension rupture, followed by shear rupture. Figure 3 shows that extensive yielding in the shear zones had already taken place by the time tension rupture occurred.

Table 1 presents a summary of the test results from this investigation. Both the peak load and the load at tension fracture are presented. With the exception of T2C, the tension rupture took place at the peak load. Specimen T2C reached its peak capacity at 90% of the displacement at which tension rupture took place.

Fig. 3. Test results for specimen T1A.**Table 1.** Test results.

Specimen	At peak load		At tension fracture		Yield strength* (MPa)	Tensile strength* (MPa)	Initial area / final area*
	Load (kN)	Deformation (mm)	Load (kN)	Deformation (mm)			
T1A	696	9.0	691	10.4	337	450	3.11
T1B	691	7.3	691	7.3	337	450	3.11
T1C	716	9.3	716	9.3	337	450	3.11
T2B	756	8.9	756	8.9	337	450	3.11
T2C	693	5.0	678	5.6	337	450	3.11

*Average value obtained from three tension coupon tests.

Finite element model

The stress distribution in gusset plates has been investigated by many researchers. Davis (1967) and Varsarelyi (1971) carried out finite element investigations of the elastic stresses in gusset plates. In general, these investigations confirmed the findings of Whitmore's (1952) experimental investigations of the stresses in gusset plates loaded in the elastic range. Inelastic analyses of gusset plates have also been conducted in a number of investigations. Williams and Richard (1986) performed numerical and experimental work to develop design procedures for gusset plate connections in frames with diagonal bracing. Their work focused on the distribution of forces in the gusset-to-frame and gusset-to-brace fasteners. Chakrabarti and Bjorhovde (1983) used a nonlinear finite element formulation to predict the structural response of gusset plates in tension. The behaviour and stress distribution in the gusset plate models were in good agreement with test results, but since the finite element formulation used for the analysis did not model buckling or material tearing, some aspects of the behaviour near ultimate load could not be compared. Walbridge et al. (1998) investigated

gusset plates subjected to monotonic loading in tension and in compression and to cyclic loading. The boundary members, brace member, and fasteners were incorporated into the model. An elastoplastic material model was used to accurately predict the peak capacity of the gusset plate in tension, although tearing of the gusset plate during tension and shear block failure was not included in the model. A similar observation was made in the work of Nast et al. (1999). Epstein and Chamarajanagar (1994) studied tension and shear block failure of angles in tension with staggered and non-staggered holes and using nonlinear solid elements. The investigators attempted to model the onset of tension and shear block failure by comparing the peak strain determined from an inelastic finite element analysis to an arbitrary strain of five times the yield strain, which was selected on the basis of a comparison of the analysis results with test results. The strains at the edge of the holes in the finite element models were calculated from the nodal displacements. The researchers reported good correlation between the finite element analyses and the test results.

For the study presented in the following, the general purpose commercial finite element analysis program ABAQUS

(Hibbitt, Karlsson & Sorenson, Inc. 2002) was used to model tension and shear block failure in gusset plates. The proposed finite element procedure is validated through comparison with results of tests presented by other researchers. A description of the development of the finite element models and the process of validating these models follows.

Preliminary analysis

The finite element model used in the preliminary analysis was based on a 9.6 mm gusset plate tested by Nast et al. (1999), the dimensional details of which are shown in Fig. 4. Although the gusset plate was mounted in a reaction frame with a beam-to-column joint, only the gusset plate was incorporated in the finite element model, with fixed boundary conditions assumed along the supported edges. Load was applied to half of each bolt hole edge surface to simulate bearing of the bolts. All the nodes that would have been under the splice plate that connected a brace member to the gusset plate were restrained in the out-of-plane direction and were free to move in the plane of the plate.

The shell element S4R from ABAQUS (Hibbitt, Karlsson & Sorenson, Inc. 2002) was used to model the gusset plate. The S4R element is a four-node doubly curved shell element that accounts for finite strains and allows for change in the element thickness. It has six degrees of freedom at each node (three displacement and three rotation components).

The analysis incorporated both geometric and material nonlinearities. The material properties used were a true stress and strain relationship derived from the average engineering stress versus strain curve obtained from tension coupon tests, as shown in Fig. 5. An isotropic hardening material model was used in the inelastic range. To capture highly localized strains and stresses that develop during necking, an additional point (point B in Fig. 5) was needed on the true stress versus strain curve beyond the ultimate stress (point A in Fig. 5). The slope of the stress versus strain curve between points A and B was obtained from the material properties of annealed A516 steel presented by Khoo et al. (2000). The material modulus in this range, as presented by Khoo et al. (2000), is 571 MPa. If the stress versus strain curve is extrapolated to a true plastic strain of 120%, the resulting stress at point B is 1200 MPa. The arc length method proposed by Riks (1979) was used for the solution strategy for the large deformation, large displacement analysis used in this study.

A mesh refinement study was conducted to determine the correct mesh size to use in the analysis. The mesh was gradually refined, and a convergence check was conducted using the major principal strains on the tension portion of the failure surface. Figure 6 shows the coarse mesh used in the mesh refinement study and Fig. 7 shows the refined mesh, in which the principal strains have converged. Because of material yielding, a high strain concentration was observed near the bolt holes, necessitating a very small mesh size. Once convergence of strains had been achieved, a comparison of the finite element analysis results with the test results was performed to validate the finite element model. The load versus deformation curve shown in Fig. 8 was used to compare the finite element result with the test result. Since the stiffness and the capacity predicted by the finite element model are in good agreement with the test results, this mesh size was used for the remaining analyses.

Fig. 4. Gusset plate tested by Nast et al. (1999). Dimensions in millimetres.

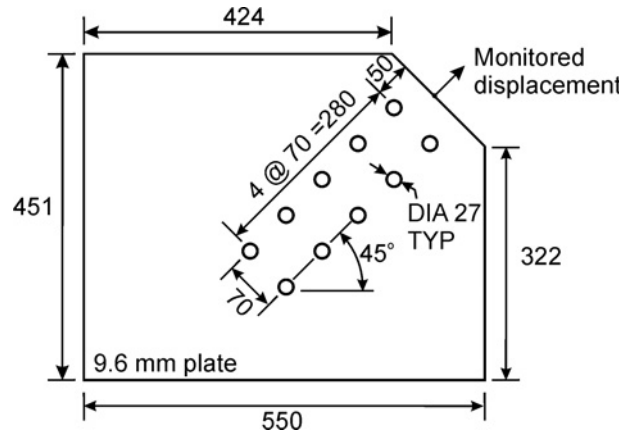


Fig. 5. Stress versus strain for gusset plate from Nast et al. (1999).

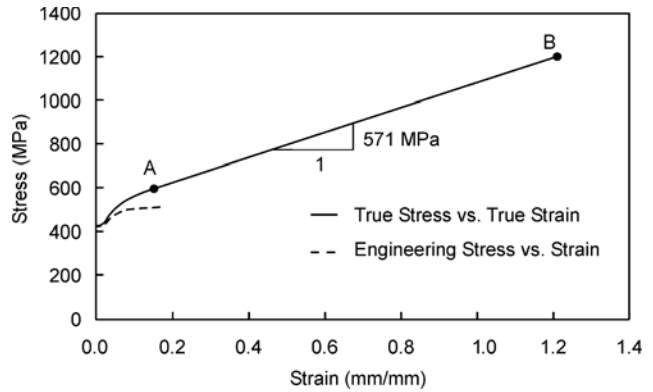
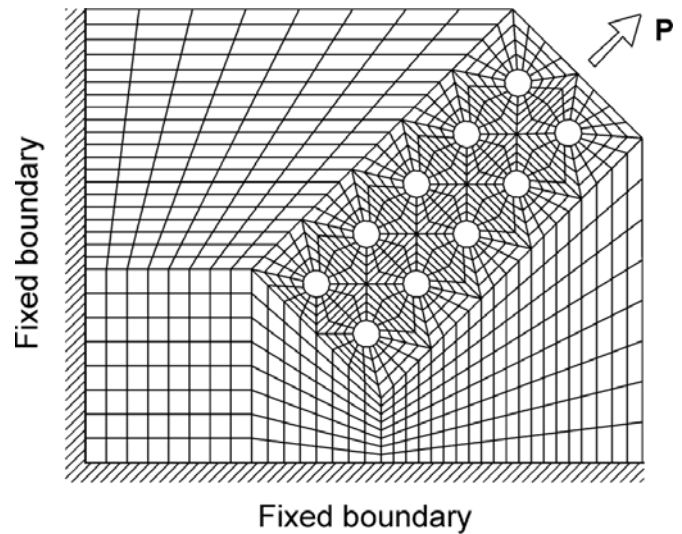


Fig. 6. Coarse mesh used in the mesh refinement study.



Modelling of fracture on the tension plane

To model the progression of rupture during tension and shear block failure, consistent failure criteria are required for the tension and shear faces of the failure surface. It was decided that the failure criterion proposed by Epstein and

Fig. 7. Fine mesh used in the mesh refinement study.

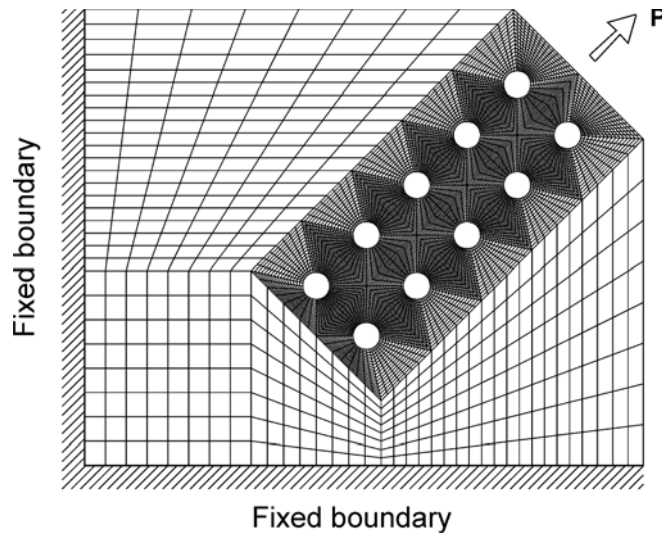
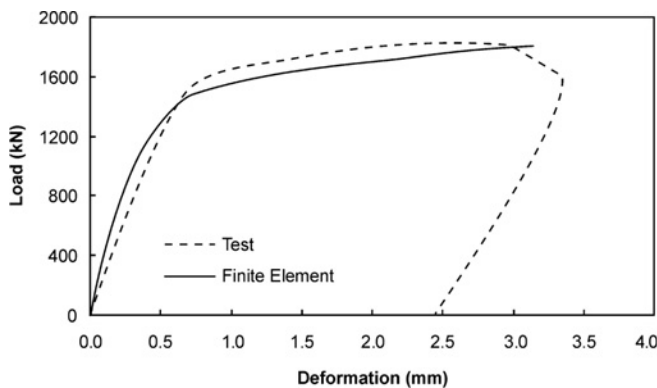


Fig. 8. Load versus deformation for fine mesh (test of Nast et al. 1999).



Chamarajanagar (1994) would not be suitable for this study because the mesh size these investigators used was much coarser than the mesh size found in the present investigation to be necessary to ensure convergence. Moreover, the rupture strain proposed by the same investigators (i.e., five times the yield strain, which would be $<1.0\%$ for this investigation) is much smaller than the rupture strain observed for structural steel. An investigation of the ductile fracture of steel by Khoo et al. (2000) showed that the localized rupture strain for structural grade steel is approximately 80% – 120% . The localized rupture strain was also obtained from tension coupon tests conducted in the experimental work described above. The true strain, or logarithmic strain, was obtained as the natural logarithm of the ratio of the initial cross-sectional area to the current area. From the tension coupon test results, the true strain at rupture was found to vary from 103% to 123% , with the average of three tension coupons being 113% . Nast et al. (1999) and other investigators cited below did not report the cross-sectional area reduction from their material tests. Therefore, a rupture strain of 100% was assumed for the validation of the finite element analysis. This represents a lower bound of the test results discussed above and an average of the values reported by Khoo et al. (2000) in their detailed investigation of these properties. To deter-

mine when fracture on the tension face would initiate, the major principal strains at the element integration points across the net tension face were plotted and extrapolated to the edge of the bolt holes by using a sixth-order polynomial. Rupture along the tension face was assumed to take place when the major principal strain at the edge of a bolt hole reached a value of 100% . Elements on the tension face were then removed from the model to simulate ductile tension fracture.

Modelling of fracture on the shear planes

Two shear fracture models were investigated. The first used a maximum principal strain of 100% as the criterion for removing elements along the shear planes. The predicted load versus displacement curve, depicted in Fig. 9, showed a sudden drop in load-carrying capacity followed by a small increase in load after tension rupture. As elements were removed on the basis of the shear rupture criterion, the load decreased again. However, as elements were deleted along the shear failure plane at larger values of connection deformation, the load started to increase again. This type of behaviour does not seem realistic, and another shear failure criterion was sought.

The second method consisted of using a critical shear strain as the rupture criterion. To establish the critical shear strain, the maximum shear strain was plotted across the tension plane at the load where the maximum principal strain had reached 100% , considered to be the localized tension rupture strain. The shear strain distribution was then extrapolated to the edge of the hole on the tension face to obtain the maximum shear strain associated with the 100% concentrated tension rupture strain. This critical maximum shear strain was subsequently used as a rupture criterion on the shear planes. When an element along the shear plane reached the critical shear strain, this element and as many as six adjacent elements along the failure path were removed. An additional iteration allowed the new equilibrium state to be reached. Load was further increased until the critical shear strain was reached once again in the next element along the failure path. The corresponding load versus deformation curve was therefore a stepped curve reflecting the stepwise nature of this crack propagation model. The loading and element removal process was repeated until the trend on the load versus deformation curve showed a significant decrease in load-carrying capacity.

Comparison of finite element analysis with test results

Test by Nast et al. (1999)

Figure 10 shows a comparison of the finite element results with those of a full-scale test conducted by Nast et al. (1999). The finite element model for this test specimen was presented in Fig. 7. Although the test was conducted under cyclic loading, the test specimen was loaded to fracture on the tension plane in the final load cycle. The finite element model was used to investigate both the pre- and post-tension fracture behaviour of the gusset plate. Since Nast et al. stopped the test at fracture of the tension face, a direct comparison between the finite element analysis and test results cannot be made beyond this point. The finite element model

Fig. 9. Load versus deformation for gusset plate tested by Nast et al. (1999), based on the criterion for principal stress – rupture on shear planes.

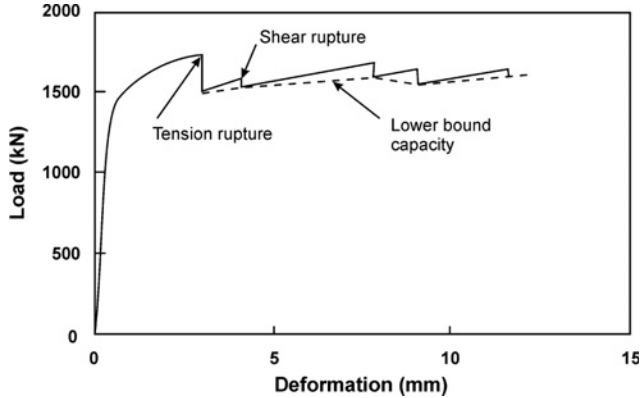
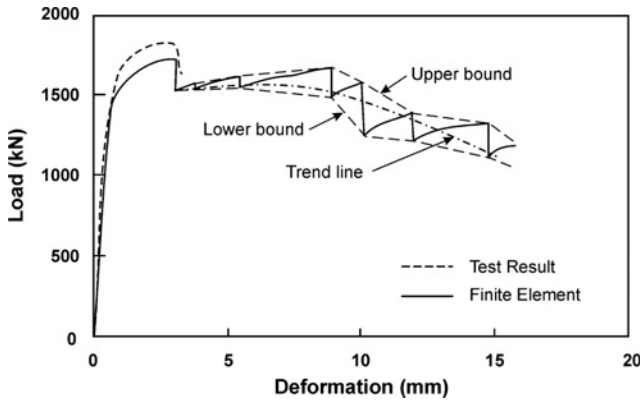


Fig. 10. Load versus deformation for gusset plate tested by Nast et al. (1999), based on the criterion for maximum shear strain – rupture.



is found to accurately predict the observed capacity of the test specimen.

The progression of the tension and shear block failure beyond tension rupture follows a general trend between the curves designated upper and lower bounds. The trend line was obtained by fitting a second-order polynomial through the load versus deformation curve obtained after tension fracture, using a least-squares regression analysis. This trend line indicates that the load-carrying capacity of the connection increases slightly after tension fracture, but it never exceeds the peak load that occurs just prior to tension fracture. The actual tension and shear block failure behaviour is characterized by the gradual tearing of the material, which can only be approximated by a series of discrete steps in the model used here.

Test by Hardash and Bjorhovde (1984)

A 6.4 mm plate (dimensions and bolt layout as shown in Fig. 11) was tested to failure by Hardash and Bjorhovde (1984). The test specimen was modelled by using a mesh (Fig. 12) similar to that used for the specimen of Nast et al. (1999). The associated stress versus strain curve is shown in Fig. 13. The modulus of elasticity was taken as 204 400 MPa, and an isotropic hardening model was used.

Fig. 11. Gusset plate tested by Hardash and Bjorhovde (1984). Dimensions in millimetres.

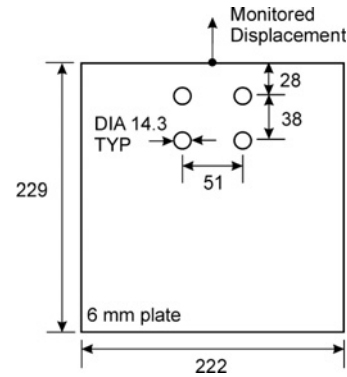


Fig. 12. Finite element model of gusset plate tested by Hardash and Bjorhovde (1984).

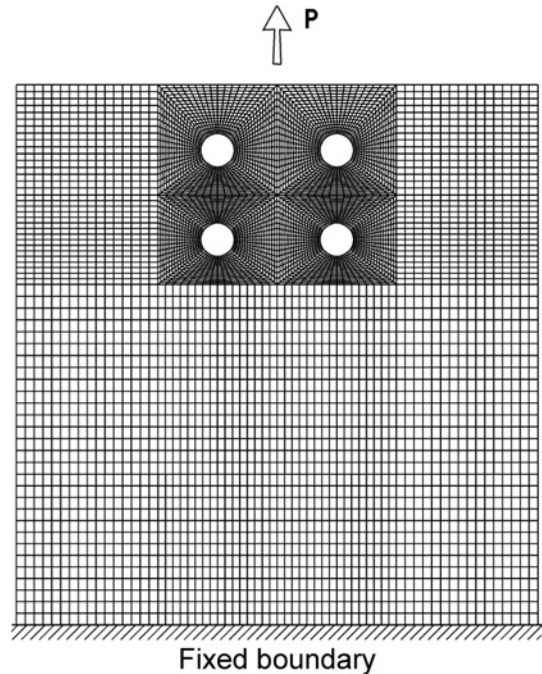
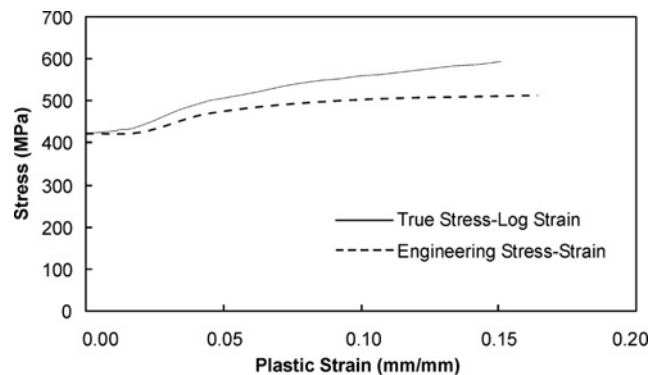
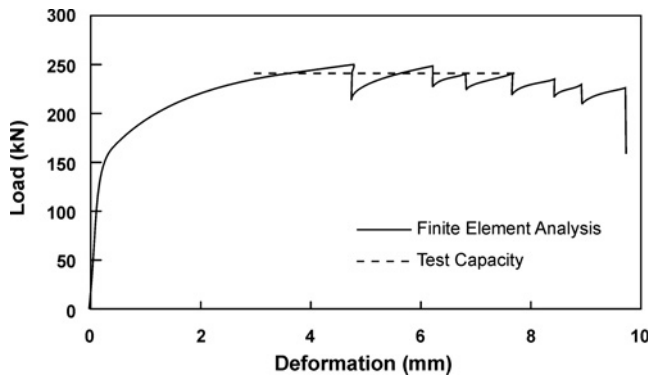


Fig. 13. Material model used for analysis of gusset plate tested by Hardash and Bjorhovde (1984).



The load versus displacement curve obtained for the Hardash and Bjorhovde (1984) specimen is shown in Fig. 14. The experimental load versus displacement curve

Fig. 14. Load versus deformation for gusset plate tested by Hardash and Bjorhovde (1984).



was not available. The general behaviour predicted by the finite element analysis is similar to that of the Nast et al. (1999) test specimen presented above. The capacity predicted with the finite element model is again in good agreement with the test result. It can be observed once again that the capacity of the gusset plate after tension fracture does not exceed the load level reached before tension rupture. The shear capacity after tension rupture either increases by a very small amount or decreases after tension rupture, indicating that all or most of the shear capacity has been mobilized by the time fracture takes place on the tension face of the tension and shear block failure surface.

Further validation of the finite element procedure

The above comparisons with test results indicate that the proposed finite element procedure is able to reliably predict the tension and shear block capacity of gusset plates. It also shows that the remaining shear capacity does not exceed the capacity developed at tension fracture in the connection configurations studied. First fracture on the tension face of the failure path can therefore reasonably be taken as an indication of the ultimate capacity of gusset plates. To further validate the finite element model developed to predict tension and shear block failure, the experimental capacities of selected test specimens were compared with the load-carrying capacities at tension rupture predicted by the proposed finite element procedure. Another nine test specimens from published and unpublished sources were analyzed, and a brief description of the specimens is presented in Table 2. The test specimens were selected to cover a wide range of geometric properties.

Each test specimen presented in Table 1 was modelled and analyzed to determine the capacity. The analysis in each case was stopped when the critical major principal strain was reached on the tension face. The shear failure progression was not investigated for these specimens. A comparison of the predicted tension and shear block capacity and the test results is presented in Table 2. The average ratio of test capacity to predicted capacity for the nine specimens presented in Table 2 is 1.04, with minimum and maximum values of 0.96 and 1.11, respectively. It is therefore concluded that the finite element model developed for tension and shear block failure is able to reliably predict the tension and shear block capacity of gusset plates.

Table 2. Verification of finite element predictions.

Source	No. of bolts	No. of lines	Edge distance (mm)	End distance (mm)	Gauge (mm)	Pitch (mm)	Plate thickness (mm)	Hole diameter (mm)	Yield strength (MPa)	Tensile strength (MPa)	Capacity (kN)		Test/ Predicted
											Test	Predicted	
University of Alberta (T1A, T1B, T1C)*	6	2	178	38	51	76	6.6	20.6	337	450	701	644	1.09
University of Alberta (T2B, T2C)*	8	4	127	25	153	51	6.5	20.6	337	450	724	692	1.05
Mullin (2005)	4	2	51	38	102	76	6.8	20.6	306	434	631	579	1.09
Mullin (2005)	8	2	52	39	103	77	7.8	21.6	306	434	1078	1009	1.07
Hardash and Bjorhovde (1984)	4	2	86	28	51	38	6.0	14.3	229	323	243	251	0.97
Hardash and Bjorhovde (1984)	6	2	118	25	102	38	6.0	14.3	229	323	375	390	0.96
Udagawa and Yamada (1998)	4	2	88	40	64	40	12.0	18.0	278	443	690	625	1.11
Udagawa and Yamada (1998)	6	2	99	40	41	40	12.0	18.0	280	444	677	664	1.02
Udagawa and Yamada (1998)	8	4	23	24	40	40	12.0	18.0	278	443	677	687	0.98

*Mean values of test results are shown in the table.

Parametric study

To expand the range of the parameters investigated experimentally, a parametric study was conducted using the finite element model presented above. From a large database of test results on gusset plates collected by Huns et al. (2002) the range of values for each parameter affecting tension and shear block capacity was obtained, as shown in Table 3. The parameters for which the ranges were increased in the parametric study are plate thickness, end distance, gauge distance, and pitch. In addition, long connections with the same number of bolts as the longest connection tested by Mullin (2005) were added to the data pool, since only one connection with eight bolts per line was tested. The next longest connection in the database of test results had five bolt per line. The five gusset plates used to expand the database of test results are described in Table 4. The plate thickness range was expanded to a maximum of 20.0 mm from 14.9 mm. The range of end distances was expanded slightly. The maximum gauge distance was extended to 150 mm from a maximum of 102 mm in the pool of experimental data. The maximum bolt pitch was almost doubled, from 76 mm investigated experimentally to 140 mm. Finally, two long connections, consisting of two lines of eight bolts, were analysed. For all the gusset plates in the parametric study, the material properties consisted of a modulus of elasticity of 198 000 MPa, a yield strength of 336 MPa, a tensile strength of 450 MPa, and a true strain at rupture of 113%.

The results of the parametric study are presented in Table 5. Plates 1 and 2 were designed for investigating whether long joints would develop substantially more load-carrying capacity beyond tension rupture. Plate 1 showed a peak load about 6% higher than the load at tension rupture, whereas plate 2, which had the same shear area as plate 1 but a larger tension area, showed no increase in capacity after fracture on the tension plane. As expected, all the other plate specimens included in the parametric study reached their maximum capacity just prior to tension rupture.

Reliability analysis

Available test results and the results of the parametric study presented above are used to assess the level of safety currently provided by design standards for gusset plates. In the development of a limit states design equation, a resistance factor (ϕ) that provides the desired level of safety is determined from a reliability analysis. The resistance factor that results from the analysis is a function of the mean values and the variabilities of the relevant material and geometric properties, as well as the ability of the equation itself to predict capacity. The resistance factor is calculated with the following equation, based on Ravindra and Galambos (1978):

$$[1] \quad \phi = \Phi_{\beta} \rho_R \exp(-\alpha_R \beta V_R)$$

where Φ_{β} is a modification factor for ϕ (discussed below); ρ_R and V_R are the bias coefficient and coefficient of variation (COV) for resistance; α_R is the separation variable for resistance; and β is the safety index, which is inversely related to the probability of failure during the life of the structure. In the limit states design approach used in North American

standards, it is desirable to have a higher safety index (lower probability of failure) for connections than for ductile structural members, such as beams. As such, members have usually been assigned a target safety index of about 3.0, whereas connections have typically been assigned a value of approximately 4.5 (Ravindra and Galambos 1978).

The bias coefficient for resistance (ρ_R) is given by the following:

$$[2] \quad \rho_R = \rho_M \rho_G \rho_P$$

where ρ_M is the ratio of the mean measured to nominal material strength; ρ_G is the ratio of the mean measured to nominal geometric properties of the connection; and ρ_P is the professional factor, or the mean ratio of measured to predicted resistance, which reflects the ability of the model to predict the capacity. The COV for the resistance (V_R) is given by the following:

$$[3] \quad V_R = \sqrt{V_M^2 + V_G^2 + V_P^2}$$

where V_M , V_G , and V_P are the COVs associated with ρ_M , ρ_G , and ρ_P , respectively.

Ravindra and Galambos (1978) recommend that the separation variable (α_R) in eq. [1] be taken as 0.55. Because of the interdependence of the resistance factor and the load factor, it has been shown by Fisher et al. (1978) that the use of a safety index other than 3.0 in eq. [1] requires that a modification factor be applied to the resistance factor. This factor, denoted as Φ_{β} here, can be expressed as follows (Franchuk et al. 2002):

$$[4] \quad \Phi_{\beta} = 0.0062\beta^2 - 0.131\beta + 1.338$$

The material factor reflects the difference between the nominal material strength (yield or ultimate) and the measured strength. The bias coefficient and the COV for the material properties were obtained from Schmidt and Bartlett (2002). Their data consisted of 1470 tension tests on plates ranging in thickness from 10.0 to 29.9 mm. Although they presented data for plate thicknesses up to 49.9 mm, only the statistics for plates up to 29.9 mm thick are used here, as this thickness is assumed to be a practical upper bound for the majority of gusset plates. The data presented by Schmidt and Bartlett consisted of static yield and tensile strengths for grade 350W steel. The bias coefficient and the COV reported by Schmidt and Bartlett (2002) for the yield strength (F_y) were 1.11 and 0.054, respectively, whereas those for the tensile strength (F_u) were 1.19 and 0.034, respectively. When equations that make use of both the yield strength and the tensile strength are being evaluated, the statistical data for F_y are used, since they are more conservative than the data for the tensile strength.

The geometric factor accounts for the difference between the nominal plate thickness and specified bolt hole layout and the actual dimensions. In the case of tension and shear block failure, the geometric factor represents the area of the tension and shear failure surfaces. Because insufficient data are available for evaluating the geometric factors, the bias coefficient and the COV for the geometric factor proposed by Hardash and Bjorhovde (1984) are used. The bias coefficient (ρ_G) and the COV (V_G) were therefore taken as 1.0 and 0.05, respectively. These values are more conservative than

Table 3. Range of gusset plate parameters investigated experimentally.

	Plate thickness (mm)	No. of bolt lines	No. of bolts per line	Bolt hole diameter (mm)	End distance (mm)	Gauge distance (mm)	Bolt pitch (mm)	Length of connection (mm)
Minimum	6.0	2	2	14.3	19.0	39.8	38.1	63.2
Maximum	14.9	4	8	27.0	63.5	102.0	76.0	570.0

Table 4. Gusset plates used in the parametric study.

Specimen	Plate thickness (mm)	No. of bolt lines	No. of bolts per line	Bolt hole diameter (mm)	End distance (mm)	Gauge distance (mm)	Bolt pitch (mm)	Length of connection (mm)
Plate 1	6.0	2	8	14.0	35.0	35.0	70.0	525.0
Plate 2	6.0	2	8	14.0	35.0	150.0	70.0	525.0
Plate 3	20.0	2	2	14.0	17.5	35.0	35.0	52.5
Plate 4	12.7	2	2	14.0	17.5	70.0	35.0	52.5
Plate 5	6.0	2	2	27.0	70.0	140.0	140.0	210.0

Table 5. Results of parametric study.

Specimen	Load at tension fracture (kN)	Ultimate load (kN)
Plate 1	1158	1230
Plate 2	1354	1354
Plate 3	618	618
Plate 4	676	676
Plate 5	815	815

the values derived by Franchuk et al. (2002) (i.e., $\rho_G = 1.017$ and $V_G = 0.039$) on the basis of measured dimensions on coped beam connections and data reported by Kennedy and Gad Aly (1980).

The ratio of the measured capacity (obtained either by laboratory testing or from a validated finite element analysis) to the capacity predicted by the equation (based on measured material and geometric properties) is used as a measure of predictability. Many equations have been proposed to predict the tension and shear block capacity of gusset plates. These equations are presented below, along with statistics (obtained by using experimental data from a large number of tests, summarized in Table 6) for the professional factor.

Equations from standard CAN/CSA-S16-01 (CSA 2001)

The Canadian steel design standard, CAN/CSA-S16-01 (CSA 2001), provides two equations for the prediction of tension and shear block capacity:

$$[5] \quad P_u = F_u A_{nt} + 0.6 F_Y A_{gv}$$

$$[6] \quad P_u = F_u A_{nt} + 0.6 F_u A_{nv}$$

where F_Y and F_u are the yield and ultimate strengths of the material; and A_{nt} , A_{gv} , and A_{nv} are the net tension, gross shear, and net shear areas, respectively. Equation [5], proposed by Kulak and Grondin (2001), is based on the observation that rupture on the tension plane occurs before rupture on the shear planes. Several test programs, including the test program presented above, support this observation.

In addition, CAN/CSA-S16-01 (CSA 2001) limits the capacity of the shear planes to the rupture strength of the net shear area, as expressed in eq. [6]. Although none of the experimental evidence presented supports this limitation, eq. [6] was adopted to provide a sufficient level of safety with a resistance factor of 0.9, which is used with eqs. [5] and [6]. Fracture on the shear planes is well known to take place on an area larger than the net area. The ratios of test values to predicted values for eqs. [5] and [6], using all the available test and finite element analysis data, are presented in the third column of Table 6. The resulting mean professional factor for all the available test results is 1.18, and the corresponding COV is 0.06.

Equations from AISC (1999) specification

The tension and shear block failure provisions in *Load and Resistance Factor Design Specification for Structural Steel Buildings* (AISC 1999) make use of two equations, the use of which is dependent on the relative strength of the net tension and shear areas of the connection:

$$\text{when } F_u A_{nt} \geq 0.6 F_u A_{nv},$$

$$[7] \quad P_u = F_u A_{nt} + 0.6 F_Y A_{gv} \leq F_u A_{nt} + 0.6 F_u A_{nv}$$

$$\text{and when } F_u A_{nt} < 0.6 F_u A_{nv},$$

$$[8] \quad P_u = F_Y A_{gt} + 0.6 F_u A_{nv} \leq F_u A_{nt} + 0.6 F_u A_{nv}$$

where A_{gt} is the gross tension area; and the other variables are as defined for CAN/CSA-S16-01 (CSA 2001). The specification uses a resistance factor of 0.75. In 108 of the 133 tests, eq. [8] governed, although rupture on the tension face was reported to occur before rupture on the shear area. Equation [8] combines the yield strength on the gross tension area with the ultimate strength on the net shear area, which was not observed in any of the 133 tests reported in Table 6, including the connections with eight transverse rows of bolts investigated numerically by Huns et al. (2002). The mean professional factor is 1.19 and the COV is 0.07, as shown in Table 6. Although eq. [8] governed in 80% of the cases investigated, the professional factor and the COV are similar to those obtained with the other models, because of the limitation imposed on the strength of the tension area,

Table 6. Ratios of test values to predicted values.

Source	No. of tests	Test/CSA-S16-01 (COV)	Test/AISC (COV)	Test/H and B (COV)	Test/Eq. [12] (COV)
Hardash and Bjorhovde (1984)	28	1.20 (0.06)	1.22 (0.06)	1.01 (0.04)	1.05 (0.05)
Rabinovitch and Cheng (1993)	5	1.22 (0.05)	1.22 (0.05)	0.99 (0.05)	0.96 (0.05)
Udagawa and Yamada (1998)	73	1.18 (0.04)	1.18 (0.05)	0.92 (0.05)	0.96 (0.06)
Nast et al. (1999)	3	1.35 (0.01)	1.35 (0.01)	1.03 (0.01)	1.00 (0.01)
Aalberg and Larsen (1999)	8	1.21 (0.03)	1.21 (0.03)	0.92 (0.07)	0.95 (0.10)
Swanson and Leon (2000)	1	1.17	1.17	0.88	0.88
Huns et al. (2002)	10	1.14 (0.15)	1.13 (0.16)	0.99 (0.08)	0.99 (0.12)
Mullin (2005)	5	1.13 (0.03)	1.15 (0.04)	1.10 (0.05)	1.02 (0.05)
Total	133	1.18 (0.06)	1.19 (0.07)	0.95 (0.07)	0.98 (0.07)

Note: CSA-S16-01, CSA (2001); AISC, AISC (1999); H and B, Hardash and Bjorhovde (1984).

which is not allowed to exceed the ultimate tensile strength on the net tension area. This condition made eq. [8] equivalent to eq. [6] in 60% of the cases. In the remaining 40% of cases, the difference between the tensile strength on the net section and the yield strength on the gross tension area was small (about 12% on average).

Provisions of AISC (2005) specification

The tension and shear block failure provisions for gusset plates in the AISC (2005) specification are identical to the provisions of CAN/CSA-S16-01 (CSA 2001) presented above.

Equation of Hardash and Bjorhovde (1984)

Hardash and Bjorhovde (1984) proposed an equation to calculate the tension and shear block capacity of gusset plates. Based on experimental observations, the equation assumes that the capacity is the sum of the ultimate strength of the net tension area plus an effective shear strength on the gross shear area. This effective shear strength is a function of the connection length (*L*) and the yield and ultimate strengths of the material. The equation is as follows:

$$[9] \quad P_u = F_u S_{net} t + 1.55 F_{eff} L t$$

where

$$[10] \quad F_{eff} = (1 - C_L) F_y + C_L F_u$$

and

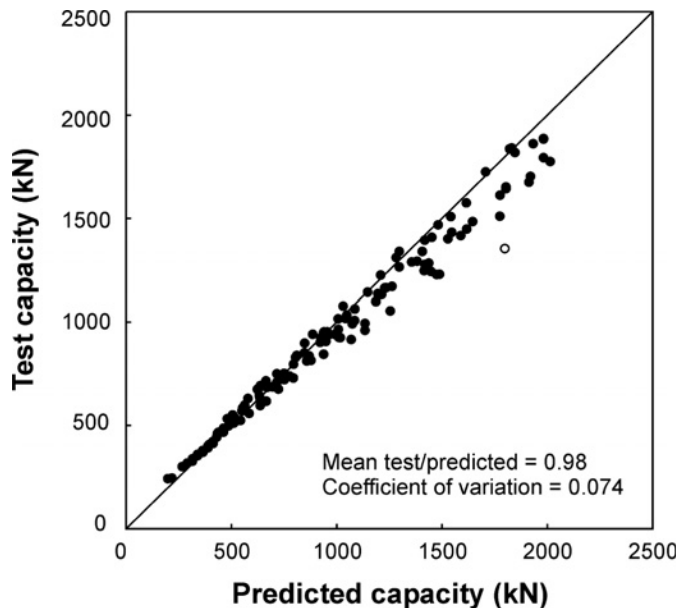
$$[11] \quad C_L = 0.95 - 0.047L$$

Although Hardash and Bjorhovde (1984) derived eq. [11] from an analysis of their own test data, eq. [9] has the advantage of offering a model that is supported by experimental observations: namely, tension fracture takes place before shear rupture, and shear failure does not take place on the net shear area. Moreover, the equation recognizes the fact that the stresses developed on the shear planes are generally significantly in excess of the shear yield stress. The mean professional factor is 0.95 and the COV is 0.07, as presented in Table 6.

Proposed equation

The equations presented above from the North American design standards generally do not give a good prediction of the tension and shear block resistance of gusset plates and

Fig. 15. Test capacity versus predicted capacity for proposed equation.



are often not consistent with the observed failure phenomenon. The equation proposed by Hardash and Bjorhovde (1984) attempts to provide a more realistic estimate of the stresses on the failure surfaces. Another equation (Driver et al. 2004) that applies to numerous connection types and is simpler in application than the Hardash and Bjorhovde (1984) equation is proposed for the design of gusset plates. The equation takes the following form:

$$[12] \quad P_u = R_t A_{nt} F_u + R_v A_{gv} \left(\frac{F_y + F_u}{2\sqrt{3}} \right)$$

where *R_t* and *R_v* are constants used to account for the non-uniformity of normal stresses on the tension area and shear stresses on the shear area, respectively. For gusset plates, Driver et al. (2004) proposed setting both constants equal to 1.0. The second term on the right hand side of eq. [12] indicates that the shear area is taken as the gross area, which is consistent with experimental observations, and the effective stress is the average of the yield strength and the tensile strength. The resulting mean professional factor is 0.98, and the associated COV is 0.07. The fact that the mean profes-

Table 7. Reliability parameters.

	Test/CSA-S16-01	Test/AISC	Test/H and B	Test/Eq. [12]
ρ_M	1.11	1.11	1.11	1.11
V_M	0.054	0.054	0.054	0.054
ρ_G	1.00	1.00	1.00	1.00
V_G	0.050	0.050	0.050	0.050
ρ_P	1.18	1.19	0.95	0.98
V_P	0.063	0.069	0.074	0.074
ρ_R	1.31	1.33	1.06	1.09
V_R	0.097	0.101	0.104	0.105
Resistance factor, ϕ				
ϕ for $\beta = 3.5$	1.04	1.04	0.83	0.85
ϕ for $\beta = 4.0$	0.97	0.97	0.77	0.79
ϕ for $\beta = 4.5$	0.90	0.90	0.71	0.73

Note: CSA-S16-01, CSA (2001); AISC, AISC (1999); H and B, Hardash and Bjorhovde (1984).

sional factor is closer to 1.0 than it is for any of the other equations considered indicates that when aggregate test data are considered, it most closely represents the failure phenomenon. Furthermore, eq. [12] provides a good representation of the observed failure mode in a large number of test specimens, namely, fracture of the net tension area before shear tearing. The equation also makes use of the gross shear area, rather than the net shear area, which is used in the American and Canadian specifications. The use of the gross shear area in eq. [12] is consistent with the observation that the failure mode observed consistently over a wide variety of tests consists of rupture on the net tension plane after yielding has occurred on the gross shear plane but prior to shear rupture on a plane that just intersects the edge of the bolt holes. It has also been demonstrated elsewhere (Driver et al. 2004) that eq. [12] leads to a consistent level of safety with elements other than gusset plates, such as coped beams, angles, and tees.

A plot of the test capacity versus predicted capacity for eq. [12] is presented in Fig. 15. The solid line represents the location where the predicted capacity is equal to the test result. Data points plotting below this line indicate that the predicted capacity exceeds the observed test capacity. The data point plotted as an open circle in Fig. 15 represents the least conservative prediction, with a test to predicted ratio of 0.75, and corresponds to plate 2 from the finite element analysis predictions of Huns et al. (2002), which is one of the longest connections in the data set. It should be noted that the model proposed by Hardash and Bjorhovde (1984) provides a test to predicted ratio of 0.86 for this test specimen. For the other 16-bolt connection investigated by Huns et al. (2002), the test to predicted ratio obtained using eq. [12] is 0.83, whereas the model of Hardash and Bjorhovde results in a test to predicted ratio of 0.97. Although these two tests seem to indicate that a length effect exists, the test by Mullin (2005) on a connection of similar length shows a test to predicted ratio of 0.96. The length effect on tension plus shear block failure is therefore inconclusive.

The professional factors by themselves do not provide a measure of the level of safety being provided by the various design equations. However, the statistical parameters de-

scribed above can be combined by using eqs. [1]–[4] to evaluate the safety index. The resistance factors required to obtain various safety index values, based on all the test results and the finite element analysis results presented in Table 6, are presented in Table 7.

Table 7 indicates that with the same resistance factor, the equations in the Canadian standard (CSA 2001) and the American design specification (AISC 1999) provide the same level of safety. A safety index of 4.5 is obtained with the current Canadian resistance factor value of 0.9. This safety index value has been adopted most often for connections. Because the Hardash and Bjorhovde (1984) model and eq. [12] provide a professional factor close to 1.0, the resistance factors required are relatively low. Table 7 shows that the target safety index of 4.5 is reached when the values of the resistance factor are 0.71 and 0.73 for the Hardash and Bjorhovde model and eq. [12], respectively. It is suggested that a resistance factor of 0.75 in conjunction with the proposed equation is appropriate, resulting in a safety index of 4.37. A resistance factor of 0.70, proposed by Franchuk et al. (2002) for coped beams, provides a safety index of 4.85.

Summary and conclusions

Although many experiments have been conducted to study tension and shear block failure in gusset plates, our understanding of the progression of fracture on the tension and shear faces is still lacking. As a result, there exists confusion about the failure progression, and failure models such as the one presented in the AISC (1999) design specification predict failure modes that are inconsistent with experimental observations. To some extent, the models used in the current design standards fail to capture the observed failure mode for tension and shear block failure.

A finite element model was developed to study the progression of tension and shear fracture in bolted gusset plates. A simple analysis technique, consisting of removing elements as fracture progresses, was developed to model ductile rupture. Tension and shear rupture criteria were proposed to model the tension and shear failures. The finite element model was validated by comparing analysis results with results from gusset plate tests. The validated finite element

procedure was then used to expand the database of test results to include a larger number of long connections, larger pitch distance, and larger gauge distance.

All the test results reported in the open literature and the finite element analyses conducted in this investigation indicate that tension fracture always occurs prior to shear rupture. Furthermore, except for unusually long and narrow connections, the full capacity of the connection is reached by the time tension rupture takes place. This supports capacity prediction models that incorporate rupture on the net tension area plus a contribution from the shear area of the concentric connection.

A reliability analysis was conducted on a database consisting of 128 test results and 5 finite element analysis results. Four models, two consisting of the design equations currently used in North American standards, an equation proposed by Hardash and Bjorhovde (1984), and an equation that was shown by Driver et al. (2004) to predict quite well the tension and shear block capacity of various connection types, were evaluated. A comparison of predicted capacities and test results indicated that the latter two equations provided a generally good prediction of the test results, whereas the equations in the two design standards underpredicted the capacities by a significant margin. Moreover, the equations in the AISC (1999) specification failed to predict the observed failure mode. All four models provided low COVs, varying from 0.063 to 0.074. Because of the high level of conservatism in the current design equations, a resistance factor of 0.90 results in a safety index of 4.5. The proposed equation, as a consequence of the mean professional factor of 0.98, requires a resistance factor of 0.74 to provide the same level of safety.

Because of its simplicity, its ability to accurately predict the tension and shear block capacity of gusset plates, its reflection of experimental observations of the failure mode, and its consistency with a previously proposed unified equation suitable for various connection types, the model expressed by eq. [12] is recommended for design. A resistance factor of 0.75 in eq. [12] provides a safety index of 4.37.

Acknowledgements

Financial support for this project was provided by the Steel Structures Education Foundation and the Natural Sciences and Engineering Research Council of Canada. This support is acknowledged with thanks.

References

- Aalberg, A., and Larsen, P.K. 1999. Strength and ductility of bolted connections in normal and high strength steels. Department of Structural Engineering, Norwegian University of Science and Technology, Trondheim, Norway.
- AISC. 1999. Load and resistance factor design specification for structural steel buildings. American Institute of Steel Construction, Chicago, Ill.
- AISC. 2005. Specification for structural steel buildings. American Institute of Steel Construction, Chicago, Ill.
- Chakrabarti, S.K., and Bjorhovde, R. 1983. Tests of full size gusset plate connections. Department of Civil Engineering, The University of Arizona, Tucson, Ariz. Research Report.
- CSA. 2001. Limit states design of steel structures. Standard CAN/CSA-S16-01, Canadian Standards Association, Toronto, Ont.
- Davis, C.S. 1967. Computer analysis of the stresses in a gusset plate. M.Sc. thesis, University of Washington, Seattle, Wash.
- Driver, R.G., Grondin, G.Y., and Kulak, G.L. 2004. A unified approach to design for block shear. Presented at the ECCS/ASCI Workshop, Connections in Steel Structures 5: Innovative Steel Connections, Amsterdam, The Netherlands, 3–4 June 2004.
- Epstein, H.I., and Chamarajanagar, R. 1994. Finite element studies for correlation with block shear tests. *Computers & Structures*, **61**: 967–974.
- Fisher, J.W., Galambos, T.V., Kulak, G.L., and Ravindra, M.K. 1978. Load and resistance factor design criteria for connectors. *ASCE Journal of the Structural Division*, **104**: 1427–1441.
- Franchuk, C.R., Driver, R.G., and Grondin, G.Y. 2002. Block shear behaviour of coped steel beams. Department of Civil and Environmental Engineering, University of Alberta, Edmonton, Alta. Structural Engineering Report No. 244.
- Hardash, S.G., and Bjorhovde, R. 1984. Gusset plate design utilizing block-shear concepts. Department of Civil Engineering and Engineering Mechanics, The University of Arizona, Tucson, Ariz.
- Hibbitt, Karlsson & Sorenson, Inc. 2002. ABAQUS/Standard. Theory manual. Version 6.2. Hibbitt, Karlsson & Sorenson Inc., Pawtucket, R.I.
- Hu, S.Z., and Cheng, J.J.R. 1987. Compressive behaviour of gusset plate connections. Department of Civil Engineering, University of Alberta, Edmonton, Alta. Structural Engineering Report No. 153.
- Huns, B.B.S., Grondin, G.Y., and Driver, R.G. 2002. Block shear behaviour of bolted gusset plates. Department of Civil Engineering, University of Alberta, Edmonton, Alta. Structural Engineering Report No. 248.
- Kennedy, D.J.L., and Gad Aly, M. 1980. Limit states design of steel structures—performance factors. *Canadian Journal of Civil Engineering*, **7**: 45–77.
- Khoo, H.A., Cheng, J.J.R., and Hrudehy, T.M. 2000. Ductile fracture of steel. Department of Civil and Environmental Engineering, University of Alberta, Edmonton, Alta. Structural Engineering Report No. 232.
- Kulak, G.L., and Grondin, G.Y. 2000. Block shear failure in steel members – a review of design practice. *In Connections in Steel Structures IV: Steel Connections in the New Millennium*, 22–25 October 2000, Roanoke, Va. American Institute of Steel Construction, Chicago, Ill.
- Kulak, G.L., and Grondin, G.Y. 2001. AISC LRFD rules for block shear—a review. *AISC Engineering Journal*, **38**(4): 199–203.
- Kulak, G.L., Fisher, J.W., and Struik, J.A.H. 1987. Guide to design criteria for bolted and riveted joints. 2nd ed. John Wiley, New York, N.Y.
- Mullin, D. 2005. Gusset plates as energy dissipaters in seismically loaded structures. Ph.D. thesis, Department of Civil and Environmental Engineering, University of Alberta, Edmonton, Alta.
- Nast, T.E., Grondin, G.Y., and Cheng, J.J.R. 1999. Cyclic behaviour of stiffened gusset plate – brace member assemblies. Department of Civil and Environmental Engineering, University of Alberta, Edmonton, Alta. Structural Engineering Report 229.
- Rabinovitch, J.S., and Cheng, J.J.R. 1993. Cyclic behaviour of steel gusset plate connections. Department of Civil Engineering, University of Alberta, Edmonton, Alta. Structural Engineering Report No. 191.
- Ravindra, M.K., and Galambos, T.V. 1978. Load and resistance factor design for steel. *ASCE Journal of the Structural Division*, **103**: 1337–1353.

- Riks, E. 1979. An incremental approach to the solution of snapping and buckling problems. *International Journal of Solids and Structures*, **15**: 529–551.
- Schmidt, B.J., and Bartlett, F.M. 2002. Review of resistance factor for steel: data collection. *Canadian Journal of Civil Engineering*, **29**: 98–108.
- Swanson, J.A., and Leon, R.T. 2000. Bolted steel connections: tests on T-stub components. *ASCE Journal of Structural Engineering*, **126**: 50–56.
- Udagawa, K., and Yamada, T. 1998. Failure modes and ultimate tensile strength of steel plates jointed with high-strength bolts. *Journal of Structural and Construction Engineering*, **505**: 115–122.
- Varsarelyi, D.D. 1971. Tests of gusset plate models. *ASCE Journal of the Structural Division*, **97**: 665–678.
- Walbridge, S.S., Grondin, G.Y., and Cheng, J.J.R. 1998. An analysis of the cyclic behaviour of steel gusset plate connections. Department of Civil and Environmental Engineering, University of Alberta, Edmonton, Alta. Structural Engineering Report No. 225.
- Whitmore, R.E. 1952. Experimental investigation of stresses in gusset plates. Engineering Experiment Station, The University of Tennessee, Knoxville, Tenn. Bulletin No. 16.
- Williams, G.C., and Richard, R.M. 1986. Steel connection design based on inelastic finite element analysis. Department of Civil Engineering and Engineering Mechanics, University of Arizona, Tucson, Ariz. Report.
- Yam, C.H.M., and Cheng, J.J.R. 1993. Experimental investigation of the compressive behaviour of gusset plate connections. Department of Civil and Environmental Engineering, University of Alberta, Edmonton, Alta. Structural Engineering Report No. 194.